

# Multiplexed Hybridization Detection with Multicolor Colocalization of Quantum Dot Nanoprobes

Yi-Ping Ho,<sup>†</sup> Matthew C. Kung,<sup>‡</sup> Samuel Yang,<sup>§</sup> and Tza-Huei Wang<sup>\*,†,‡</sup>

*Department of Mechanical Engineering, Department of Biomedical Engineering, and Department of Emergency Medicine, The Johns Hopkins University and School of Medicine, Baltimore, Maryland 21218*

*Received May 12, 2005; Revised Manuscript Received June 27, 2005*

## ABSTRACT

We demonstrate a hybridization detection method using multicolor oligonucleotide-functionalized quantum dots as nanoprobes. In the presence of various target sequences, combinatorial self-assembly of the nanoprobes via independent hybridization reactions leads to the generation of discernible sequence-specific spectral codings. Detection of single-molecule hybridization is achieved by measuring colocalization of individual nanoprobes. Genetic analysis for anthrax pathogenicity through simultaneous detection of multiple relevant sequences is demonstrated using this novel biosensing method as proof-of-concept.

Sequence-specific nucleic acid detection has become a pervasive theme in a variety of biomedical disciplines such as disease diagnosis and treatment, forensic analysis, and biodefense strategy. Although still in its infancy, the application of surface-functionalized nanomaterials such as nanoparticles in sequence recognition schemes has shown great promise in achieving high sensitivity (e.g., zeptomole sensitivity<sup>1</sup>) and specificity (e.g., selectivity factor of  $\sim 100000:1^2$ ), which are difficult to achieve by conventional methods. Driven by the need to analyze an ever-increasing number of target sequences in a complex mixture, current efforts have been focused on the development of addressable DNA nanosensors (e.g., metallic Au nanoparticles<sup>3–5</sup> and multi-metal nanorods<sup>6</sup>) capable of measuring multiple targets in parallel.

Semiconductor quantum dots (QDs),<sup>7,8</sup> with their unique photophysical properties such as narrow and size-tunable emission spectra, robust signal intensity, broad excitation bandwidth, and high photochemical stability against photobleaching, have been shown to be ideal for use as spectral labels in multiplexed bioanalysis.<sup>9,10</sup> Multicolor optical “bar codes” have been generated by embedding different sized QDs into microbeads at precisely controlled ratios. Conjugated with oligonucleotide probes in a hybridization assay, the encoded microbeads have enabled multiplexed target

recognition and identification to occur in a separation-free, solution phase detection format which has faster binding kinetics and simpler assay protocol than separation-dependent detection on a solid phase.<sup>11,12</sup> In this QD-microbead based detection format, however, an additional organic fluorophore is often required for labeling and quantification of the target analyte. As a result, analysis in the setting of low target abundance can be limited by weak target signals, as these are difficult to detect against the strong coding signal of the nearby microbead that is comprised of approximately tens of thousands of QDs.

In this paper, we report an alternative separation-free multiplexed detection method capable of detecting low-abundance DNA targets, based on multicolor colocalization of target-specific QD nanoprobes (i.e., QDs surface-functionalized with oligonucleotide probes) upon hybridization (Figure 1a). The use of QDs as fluorescent tags allows unambiguous colocalization analysis of single-molecule probes.<sup>13,14</sup> Two QD nanoprobes, each with discernible emission wavelengths, are designed to bind in juxtaposition to the same target DNA of interest to form a sandwiched nanoassembly. Since the physical size of the nanoassembly ( $\sim 50$  nm) is smaller than the diffraction-limited resolution ( $\sim 250$  nm) of an optical imaging system, the nanoassembly is imaged as a combined color due to spatial colocalization of the two linked QD nanoprobes. As a result, target presence can be determined based on colorimetric measurements of the nanoassemblies, and multiplexed sequence identification can be achieved through the use of multiple combinations of different-color QD nanoprobes (Figure 1b). Different from

\* Corresponding author: e-mail, thwang@jhu.edu; tel, (410) 516-7086; fax, (410) 516-7254.

<sup>†</sup> Department of Mechanical Engineering, Johns Hopkins University.

<sup>‡</sup> Department of Biomedical Engineering, Johns Hopkins University.

<sup>§</sup> Department of Emergency Medicine, Johns Hopkins School of Medicine.

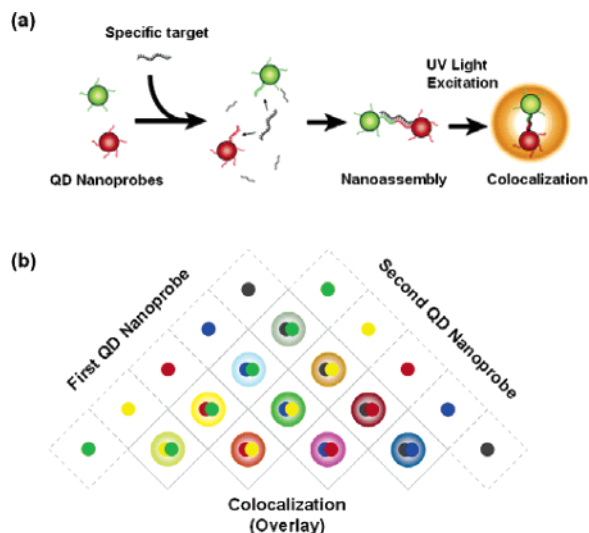


**Figure 1.** (a) QD nanoprobes prepared by surface-functionalizing QDs with target-specific oligonucleotide probes. Two target-specific QD nanoprobes with different emission wavelengths sandwich a target, forming a QD probe–target nanoassembly. The nanoassembly is detected as a blended color (orange) due to the colocalization of the both QD nanoprobes. (b) The color combination scheme for multiplexed colocalization detection.

the multiplexing schemes using QD<sup>11,12</sup> or fluorophore<sup>15</sup> embedded microbeads as spectral bar codes, the target-specific codings in our method are naturally generated upon independent sandwich hybridizations in the presence of different targets. With this method,  $n$  different QDs can each be used for conjugation of  $(n - 1)$  different oligonucleotide probes to prepare  $n(n - 1)$  QD nanoprobes capable of simultaneously detecting  $\frac{1}{2}n(n - 1)$  targets. Since the unbound QD probes retain their original colors and the hybridized nanoassemblies display a variety of combined colors, both the QD probes and hybridized nanoassemblies are easily differentiated from each other, negating the need for a solid-phase support for separation of the unbound probes.

To demonstrate the colocalization detection method, we first used simply one oligonucleotide target (5′-ACG GCA GAC TTC TCC TGA GGA GTC AGG TGC AC-3′) with two QD nanoprobes (P1: 5′-/525QD (peak emission at 525 nm)/GTG CAC CTG ACT CCT C-3′, P2: 5′-AGG AGA AGT CTG CCG T/605QD (peak emission at 605 nm)/-3′). QD nanoprobes were prepared by conjugating biotinylated oligonucleotide probes to streptavidin-functionalized QDs. Excess probes were used in the reaction to achieve high surface coverage of oligonucleotides to stabilize the QDs against aggregation. The sample was analyzed in a wide-field fluorescence microscope capable of single-particle detection. As shown in Figure 2b, in the presence of specific targets, orange nanoassemblies (pseudocombined color) were observed in addition to those of free QD nanoprobes in green (525QD) and red (605QD). Colocalization of the QD nanoprobes was also verified by analyzing the three-dimensional (3-D) contour of the fluorescent signals in the two separate color panels (Figure 2c). To verify the detection specificity and analyze the background signal level from

nonspecific hybridization, we conducted a negative control experiment by analyzing colocalization of QD nanoprobes in the presence of target-free genomic DNA from *Escherichia coli*. As shown in the representative fluorescent image in Figure 2a, colocalized orange fluorescence was barely observed throughout the entire field of view (FOV, 90  $\mu$ m by 67  $\mu$ m). Furthermore, the number of colocalized QD nanoprobes and noncolocalized free QD nanoprobes detected in both the negative control and the sensing experiment (with specific targets presence) were analyzed and compared (parts d and e of Figure 2). The colocalization percentage, defined as the number of colocalized QD nanoprobes divided by the total number of QD nanoprobes (in the 605QD channel), was measured to be <1% in the negative control and ~25% in the sensing experiment. The distinct difference in the colocalization percentage between both experiments demonstrates a high specificity with the sandwich hybridization/colocalization detection method.

Several lines of evidence suggest that single units of nanoassemblies were detected. First, the absence of colocalized fluorescent spots in the negative control (Figure 2a) suggests that target-independent aggregation of QD nanoprobes was minimal and the observed discrete fluorescent spots stemmed mainly from individual free QD nanoprobes. Second, the discrete luminescence signals showed intermittent on/off or “blinking” behavior, which was similar to the behavior reported for single CdSe QDs.<sup>8</sup> Third, we analyzed the histograms of fluorescence intensity (in the 605QD channel) detected in free QD nanoprobes versus hybridized nanoassemblies (Figure 3). The distribution of nanoassemblies is wider and long-tailed, suggesting that a portion of nanoassemblies was comprised of more than one pair of hybridized QD nanoprobes. However, there was also a substantial overlap with that of the free QD nanoprobes, indicating that a large fraction of the nanoassemblies were comprised of single pairs of hybridized QD nanoprobes. These results suggest that our detection system is capable of detecting hybridization events at the most fundamental level.

To demonstrate the potential biological application of our detection system, we chose to design a prototype assay based on multicolor-colocalization of QD nanoprobes for the genetic analysis of anthrax pathogenicity. To positively identify a pathogenic strain of *Bacillus anthracis*, simultaneous detection of three genes, namely *rpoB*, *pagA*, and *capC*, is required.<sup>16</sup> *RpoB* is a chromosomal marker with species–species sequences which can be used to differentiate *B. anthracis* from other *Bacillus* species, while *pagA* and *capC* are the plasmid markers for determining the presence of anthrax toxin. As proof of concept, three synthetic oligonucleotides, each derived from conserved sequences from each of the three anthrax-related genes, were used as simulated targets (in a background of *E. coli* genomic DNA) for analysis with three pairs of target-specific probes conjugated combinatorially to three QDs with distinct emission wavelengths: 525QD, 605QD, and 705QD (peak emission at 705 nm) (Table 1). The detection of fluorescent spots in the combined pseudocolors, namely, indigo, ma-

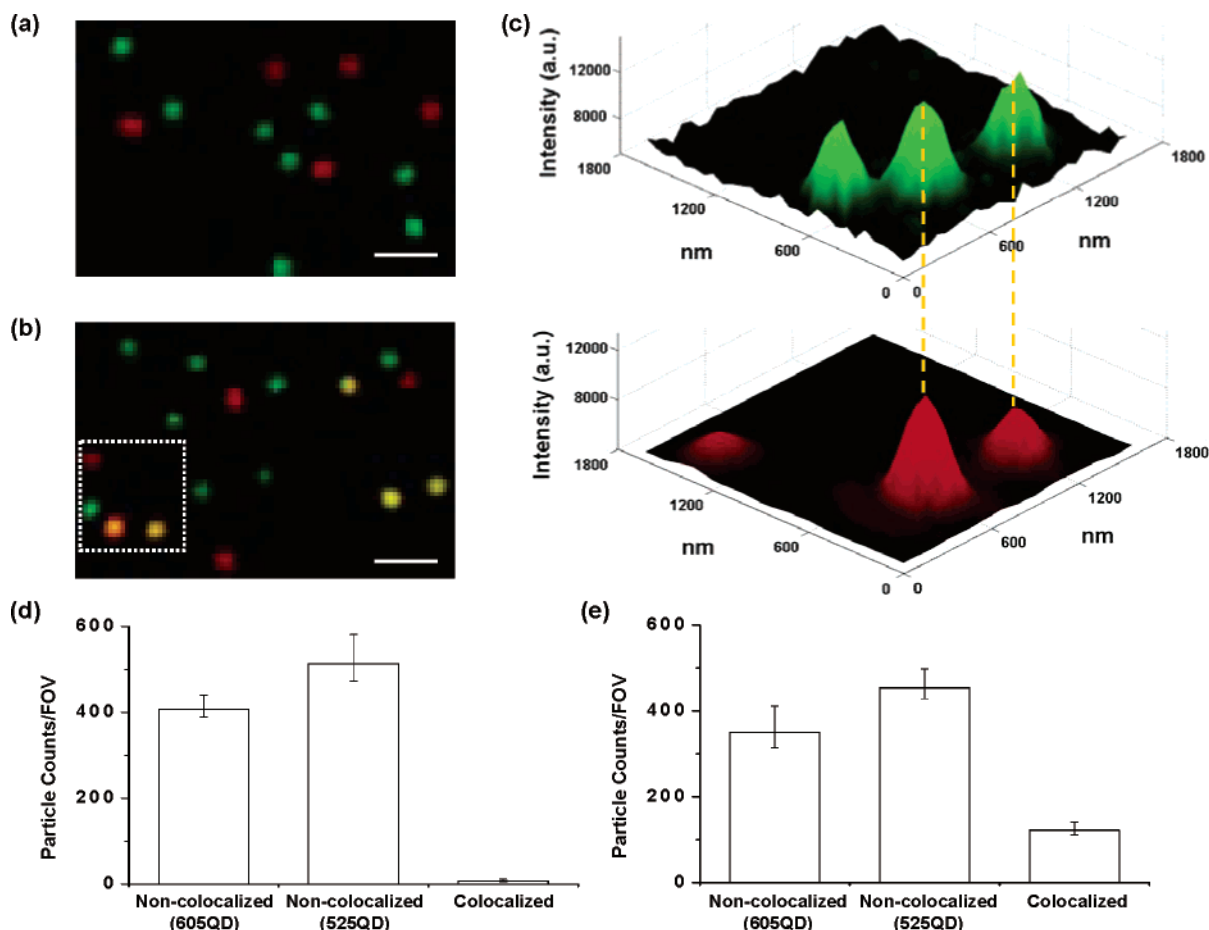


**Figure 2.** (a) In a sample containing background bacterial genomic DNA, only discrete green and red fluorescent spots from unhybridized QD nanoprobes ( $10^{-10}$  M) are measured in the negative control experiment. (b) In the presence of specific targets ( $10^{-10}$  M), colocalized fluorescent spots appear as a blended orange color, indicating the formation of nanoassemblies upon sandwich hybridization. (c) 3D contours from the range of interest (ROI) in (b) are analyzed for both green and red channels. The dashed lines indicate the colocalization of the green and red fluorescent signals. (d and e) The number of colocalized QD nanoprobes and noncolocalized QD nanoprobes counted per FOV in the negative control (d) and the sensing experiment (e). Error bars were determined based on three measurements. (Bar dimension is  $1 \mu\text{m}$ .)

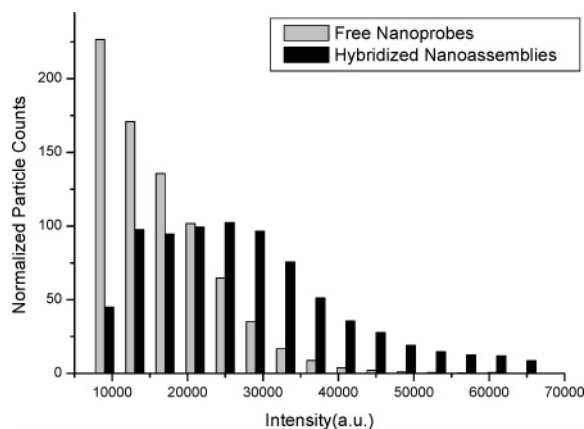


**Figure 3.** Histogram of particle fluorescence intensity distribution in the red emission wavelength (605 nm) from both free QD nanoprobes and hybridized nanoassemblies.

genta, and orange, signifies the presence of *rpoB*, *pagA*, and *capC*, respectively (Figure 4a). Four series of experiments were conducted to evaluate the specificity of the assay by its capacity to correctly identify and quantify the individual target sequences in a complex mixture of various target

**Table 1.** Sequences of the Three Anthrax-Related Targets (*rpoB*, *capC*, and *pagA*) and Their Associated Oligonucleotide Probes

Denomination	Sequences	Position
<i>rpoB</i> (AF205326)	5'- ACT TGT GTC TCG TTT CTT CGA TCC AAA GCG -3'	350-379
<i>rpoB</i> Probe1	3'-/QD525 ● - TGA ACA CAG AGC AAA - 5'	
<i>rpoB</i> Probe2	3'- GAA GCT AGG TTT CGC - /QD705 ● - 5'	
<i>capC</i> (M24150)	5'- ATG CCA TTT GAG ATT TTT GAA TTC CGT GGT -3'	1781-1810
<i>capC</i> Probe1	3'-/QD605 ● - TAC GGT AAA CTC TAA - 5'	
<i>capC</i> Probe2	3'- AAA CTT AAG GCA CCA - /QD705 ● - 5'	
<i>pagA</i> (M22589)	5'- CTC GAA CTG GAG TGA AGT GTT ACC GCA AAT -3	3312-3341
<i>pagA</i> Probe1	3'-/QD525 ● - GAG CTT GAC CTC ACT -5'	
<i>pagA</i> Probe2	3'- TCA CAA TGG CGT TTA - /QD605 ● - 5'	

combinations (Figure 4b). In the first experiment (Figure 4c, I), fluorescent spots in all the three combined pseudocolors were detected, verifying the presence of the three targets in the solution. In the next two experiments, the presence of two (Figure 4c, II) or only one (Figure 4c, III) target was also unambiguously determined without false positive or negative results. In the negative control sample in which

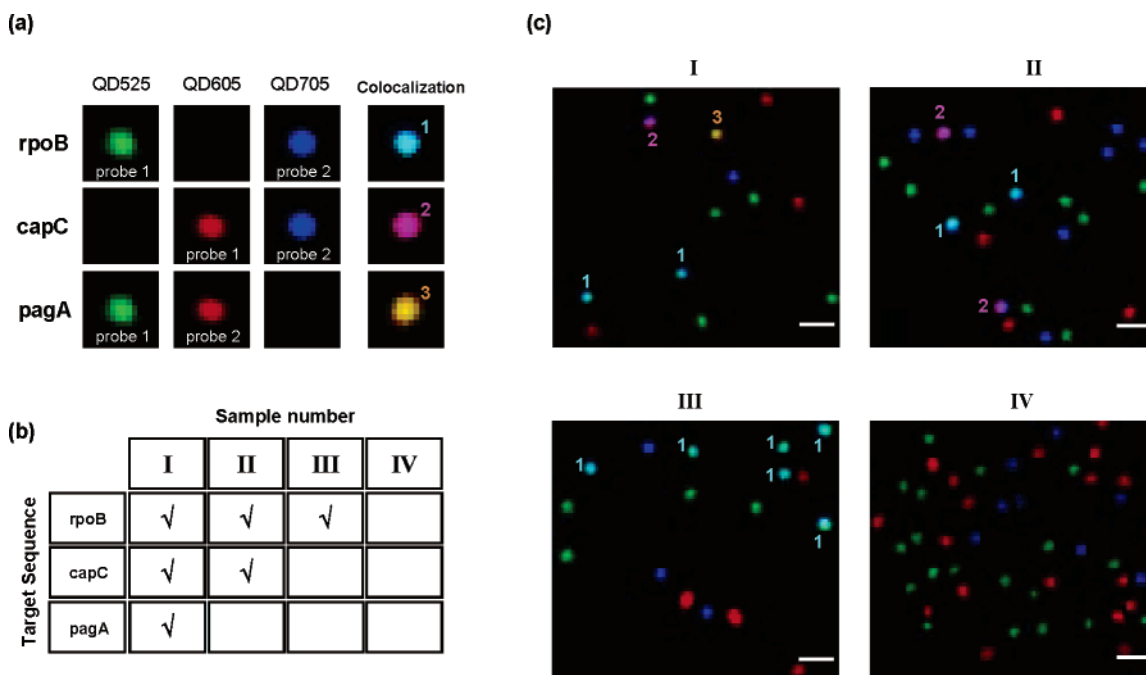


**Figure 4.** Simulated multiplexed analysis of anthrax-related genetic targets for pathogenicity: (a) color pallet for the three pairs of target-specific QD nanoprobe and their resulting colocalized fluorescent images upon sandwich hybridization; (b) four samples containing different combinations of the three targets, rpoB, capC, and pagA. Checks represent the existence of certain target sequences. Sample IV does not contain any target and is used as a negative control. (c) Fluorescent images I, II, III, and IV correlate with samples I, II, III, and IV, respectively. (Bar dimension is 1  $\mu\text{m}$ .)

specific targets were absent (Figure 4c, IV), only fluorescent spots stemming from unhybridized blue, green, and red QD nanoprobe were observed. It is worthwhile to note that a single wavelength light source was used for all the experiments which is difficult to achieve in an organic fluorophore-based multiple color fluorescence microscopy.

One requirement for optimizing the performance of the multicolor colocalization detection method is that the QDs used in the assays must have distinct emission wavelengths. Up to 10 QDs with distinguishable emissions wavelengths have been demonstrated to be simultaneously observed upon excitation by a single wavelength light source.<sup>12,17</sup> The use of 10 distinct QDs in the multicolor color colocalization method could allow simultaneous detection of up to 45 different targets in a combinatorial approach. It is possible to further increase the multiplexing capacity by using additional QDs with infrared emissions. Another requirement for optimal performance is that a low concentration of QD nanoprobe should be used in order to minimize the false positive detection caused by statistical colocalization of QD nanoprobe. The measured statistical colocalization of free QD nanoprobe is lower than 1% when measuring the QD nanoprobe at  $<1$  nM. While the use of low probe concentrations for hybridization reactions could potentially lead to prolonged hybridization time, we observed complete hybridization within 60 min (see Supporting Information). The enhanced hybridization kinetics may be attributed to the homogeneous nature (both hybridization and detection take place in a solution phase) of our detection method.

In summary, we have reported a multiplexed hybridization detection method in a homogeneous, separation-free format based on multicolor colocalization of oligonucleotide-func-

tionalized QD nanoprobe. Imaging experiments indicate that this method is capable of detecting DNA hybridization at the single molecule/particle level and is therefore ideal for analyzing low-abundance targets. In addition, the hybridized and unhybridized strands can be differentiated and quantified through colorimetric measurements and particle counting. This offers great promise for quantitative study of molecular binding kinetics. Finally, as proof of concept, multiplexed detection of three target sequences derived from *B. anthracis*-related genes has been demonstrated with high sensitivity and specificity. Ultimately, the described method can serve as a generic biosensing platform whose application can later be extended to detect other types of bioparticles (e.g., proteins) by conjugating QDs with different molecular probes (e.g., antibody).

**Acknowledgment.** This work is supported by NSF under Award No. DBI-0352407 and Whitaker Foundation.

**Supporting Information Available:** Experimental methods. This material is available free of charge via the Internet at <http://pubs.acs.org>.

## References

- (1) Storhoff, J. J.; Lucas, A. D.; Garimella, V.; Bao, Y. P.; Muller, U. R. *Nat. Biotechnol.* **2004**, *22*, 883–887.
- (2) Park, S.-J.; Taton, T. A.; Mirkin, C. A. *Science* **2002**, *295*, 1503–1506.
- (3) Taton, T. A.; Lu, G.; Mirkin, C. A. *J. Am. Chem. Soc.* **2001**, *123*, 5164–5165.
- (4) Bailey, R. C.; Nam, J. M.; Mirkin, C. A.; Hupp, J. T. *J. Am. Chem. Soc.* **2003**, *125*, 13541–13547.
- (5) Cao, Y. C.; Jin, R.; Mirkin, C. A. *Science* **2002**, *297*, 1536–1540.
- (6) Nicewarner-Pena, S. R.; Freeman, R. G.; Reiss, B. D.; He, L.; Pena, D. J.; Walton, I. D.; Cromer, R.; Keating, C. D.; Natan, M. J. *Science* **2001**, *294*, 137–141.

- (7) Bruchez, M.; Moronne, M.; Gin, P.; Weiss, S.; Alivisatos, A. P. *Science* **1998**, *281*, 2013–2016.
- (8) Chan, W. C. W.; Nie, S. M. *Science* **1998**, *281*, 2016–2018.
- (9) Gerion, D.; Parak, W. J.; Williams, S. C.; Zanchet, D.; Micheel, C. M.; Alivisatos, A. P. *J. Am. Chem. Soc.* **2002**, *124*, 7070–7074.
- (10) Robelek, R.; Niu, L. F.; Schmid, E. L.; Knoll, W. *Anal. Chem.* **2004**, *76*, 6160–6165.
- (11) Xu, H. X.; Sha, M. Y.; Wong, E. Y.; Uphoff, J.; Xu, Y. H.; Treadway, J. A.; Truong, A.; O'Brien, E.; Asquith, S.; Stubbins, M.; Spurr, N. K.; Lai, E. H.; Mahoney, W. *Nucleic Acids Res.* **2003**, *31*, e43.
- (12) Han, M. Y.; Gao, X. H.; Su, J. Z.; Nie, S. *Nat. Biotechnol.* **2001**, *19*, 631–635.
- (13) Lacoste, T. D.; Michalet, X.; Pinaud, F.; Chemla, D. S.; Alivisatos, A. P.; Weiss, S. *Proc. Natl. Acad. Sci. U. S. A.* **2000**, *97*, 9461–9466.
- (14) Michalet, X.; Lacoste, T. D.; Weiss, S. *Methods* **2001**, *25*, 87–102.
- (15) Fulton, R. J.; McDade, R. L.; Smith, P. L.; Kienker, L. J.; Kettman, J. R. *Clin. Chem.* **1997**, *43*, 1749–1756.
- (16) Ellerbrok, H.; Nattermann, H.; Ozel, M.; Beutin, L.; Appel, B.; Pauli, G. *FEMS Microbiol. Lett.* **2002**, *214*, 51–59.
- (17) Chan, W. C. W.; Maxwell, D. J.; Gao, X. H.; Bailey, R. E.; Han, M. Y.; Nie, S. M. *Curr. Opin. Biotechnol.* **2002**, *13*, 40–46.

NL050888V